**ORIGINAL ARTICLE**

# The effects of MgS nanoparticles-Cisplatin-bio-conjugate on SH-SY5Y neuroblastoma cell line

Ozge Balpinar Nalci[1] · Hayrunnisa Nadaroglu[2,3] · Sidika Genc[4] · Ahmet Hacimuftuoglu[4] · Azize Alayli[5]

## Abstract

Magnesium sulfide nanoparticles (MgS NPs) is a nanomaterial that has an important place in diagnosis, treatment, diagnosis, and drug delivery systems. Neuroblastoma, a type of brain cancer, is an extremely difficult cancer to treat with today's treatment options. This study was carried out to determine the cytotoxic, oxidant, and antioxidant effects on the neuroblastoma cancer line (SH-SY5Y cell line) along with the green synthesis and characterization of MgS NPs structures. MgS NPs were synthesized by green synthesis using $Na_2S$ and *Punica granatum*, a cleaner method for toxic effects, and characterized using Scanning Electron Microscopy, Fourier Transform Infrared spectroscopy, X-Ray diffraction methods. In cell culture, SH-SY5Y cells were grown in a suitable nutrient medium under favorable conditions. Five different doses of MgS NPs (10, 25, 50, 75, and 100 µg/mL) were applied to the cell line for 24 h. The analysis of the MgS NPs applications was performed with MTT cytotoxicity test and total oxidant and total antioxidant tests. According to the data obtained, 75 µg/mL MgS NPs application decreased cancer cell viability up to 48.54%. MgS NPs exhibited a dose-dependent effect on the SH-SY5Y cell line. Also, it was determined that MgS NPs increased oxidant activity in neuroblastoma cells, which was compatible with the cytotoxicity test. As a result, MgS NPs exhibited an effective activity on the neuroblastoma cell line. It was clearly seen that NPs obtained by green synthesis prevented the related cancer line from proliferating.

**Keywords** MgS Nanoparticles · Bio-conjugate · Cisplatin · SH-SY5Y neuroblastoma cell lines

## Introduction

Located in metallic nanoparticles, MgS has a wide range of applications in biomedicine [1]. Compared to Bulk form, the uniqueness of the physicochemical properties of MgS NPs such as the presence of high-energy atoms in the surface area of the particles, high surface area volume ratio is one of the main reasons for being preferred in applications [2, 3]. It is seen that these nanoparticles have been tested in many published studies in areas such as diagnosis, drug transportation, anti-cancer activity, anti-microbial activity, anti-inflammatory activity, and disease treatment [4, 5].

Many metallic nanoparticles are effective in reducing the proliferation of cancer cells. It is known that anticancer effects occur with many different mechanisms. It has been determined that the anticancer effect of AgNPs on colon cancer cells occurs by activation of p53-mediated apoptotic changes [6]. The antiproliferative effects of most metal nanoparticles are due to cytotoxicity caused by high levels of reactive oxygen species [5, 7–9].

Drug binding to metallic nanoparticles is carried out in two ways; drug binding at the molecular level or binding of the drug to the surface. Molecular drug binding methods include processes such as physical complexing, dendrimer complexing, chemical bonding with polymer-based prodrugs. The process of binding the drug to the surface

✉ Hayrunnisa Nadaroglu
hnisa25@atauni.edu.tr

✉ Ahmet Hacimuftuoglu
ahmeth@atauni.edu.tr

1  Department of Medical Pharmacology, Faculty of Medicine, Ondokuz Mayıs University, Samsun, Turkey

2  Department of Food Technology, Erzurum Vocational College, Ataturk University, 25240 Erzurum, Turkey

3  Department of Nano-Science and Nano-Engineering, Institute of Science and Technology, Ataturk University, 25240 Erzurum, Turkey

4  Department of Medical Pharmacology, Faculty of Medicine, Ataturk University, Erzurum, Turkey

5  Department of Nursing, Faculty of Health Sciences, Sakarya University of Applied Sciences, 54187 Sakarya, Turkey

is based on two factors, basically the surface-volume ratio and the physicochemical properties of the surface [10].

Neuroblastoma, which is frequently involved in scientific studies, is seen as an extra-cranial solid tumor, which is encountered in childhood. It has an annual incidence of 10.54 per million in children under 15 years of age, one in every 7000 live births [11]. Its treatment is carried out with alkylating agents such as cisplatin. However, since the common cytotoxic effect of drugs such as cisplatin causes severe side effects, there is a need to develop new approaches in the treatment of neuroblastoma [12]. It is stated that even smarting agents encapsulated with nanoformulations exhibit more effective and safer developments compared to cisplatin alone. It is observed that neuroblastoma cancer does not recur in most of the in vitro and in vivo studies performed in this direction. [13, 14] For this reason, nanomedicine is the answer to the need for less toxic and more effective treatment options.

It is known that MgO NPs have anticancer activity on the K562 cancer line. It performs this activity without harming human serum albumin (HSA) and PBMC cells [15]. However, the anticancer efficacy of MgS NPs for each cancer line has not been investigated. With this study, green synthesis of MgS NPs was performed and characterization of nanoparticles was performed. Subsequently, this study investigating the effectiveness of MgS NPs on the neuroblastoma cancer line is a first in terms of providing new data to the literature.

## Materials and methods

### Chemicals

The supply of Cisplatin from Kocak Pharma Ltd (Tekirdag, Turkey) was provided. Amlodipine, fetal calf serum (FCS), Dulbecco Modified Eagles Medium (DMEM), phosphate buffer solution (PBS), L-glutamine, trypsin–EDTA, and antibiotic antimitotic solution (×100) were acquired from Sigma Aldrich (St. Louis, USA) MO, United States.

### Preparation of plant extract

*Punica granatum* fruits were purchased from local markets in Erzurum, Turkey, and it was identified with the helping of taxonomists. After pomegranate seeds were picked, 25 g pomegranate seeds were crushed in 100 ml of pure water with the help of a grinder. It was first filtered by filter paper, then centrifuged at $5000 \times g$ for 10 min, and the supernatant was used for green synthesis.

### Green synthesis and characterization of MgS NPs

MgS NPs were firstly synthesized using *Punica granatum* fruit extract and determination of surface topography MgS NPs was performed by Scanning Electron Microscope (SEM) (Zeiss Sigma 300 microscope, Carl Zeiss AG, Jena, Germany). The surface morphologies of the MgS-NPs were examined using a Metek, Apollo prime, active area 10 mm$^2$, Microscope inspect S50. Then, X-ray diffraction (XRD) analysis was determined in the determination of the crystallinity of MgS NPs by PANalytical EMPYREAN XRD (Malvern Panalytical Inc., Westborough, MA, USA). X-ray diffraction patterns were performed on Panalytical empyrean equipped with Ni-filtered Cu Kα radiation ($\lambda = 0.1542$ nm) in the range of 10–80° at a scanning rate of 4° min$^{-1}$. FT-IR analysis of MgS NPs was recorded using Vertex 80 Model FT-IR Frontier spectrophotometer (Bruker Ltd., Karlsruhe, Germany) with attenuated total reflection (ATR) technique in the 4000–400 cm$^{-1}$ region [16–18].

### Cell culture

Neuroblastoma cell lines from the Ataturk University Medical Pharmacology department (Erzurum, Turkey) were obtained. The growth and development of cells were accomplished with Dulbecco's Modified Eagle Medium supplemented with F12 medium (Euroclone, Milano, Italy) containing 10% Fetal Bovine Serum (Euroclone, Milano, Italy) and 0.1% Penicillin/Streptomycin. The cells were developed by keeping them at 37 °C in an environment containing 5% CO$_2$. Nanoparticle application was performed after the cells reached to 85% confluency level. MgS NPs were administered in five different doses (10, 25, 50, 75 and 100 µg/mL) in four replicates, in a positive and negative controlled manner.

### Morphological imaging

Morphological changes occurring in the cells were visualized with an inverted microscope (Leica Microsystems, Wetzlar, Germany). The images obtained were recorded with ×200 magnification of the microscope.

### MTT assay

After 24 h on cells treated with nanoparticles, the administration was terminated, and the MTT cytotoxicity test was performed. The plates containing the applications were kept for 4 h in an environment containing 5% CO$_2$ at 37 °C with MTT solution. To dissolve the formazan crystals formed as a result of MTT, 100 µL DMSO was added to each well. To determine

the density of formazan crystals, data were obtained by reading plates with Multiskan ™ GO Microplate Spectrophotometer reader at a wavelength of 570 nm [19].

## Total oxidant status (TOS) and total antioxidant capacity (TAC) analysis

Since oxidant and antioxidant effects are collectible, the effects of these molecules are measured collectively due to the difficulty of individual measurement of different oxidant and antioxidant substances [20]. Total Antioxidant Capacity (TAC) and Total Oxidant Status (TOS) analyzes were performed with cell culture fluids obtained after application. In this respect, utilizing commercially available kits may be data that was obtained (Rel Assay Diagnostics, Bursa, Turkey).

## Real-time cell cytotoxicity assay

xCELLigence ™ Real-Time Cell Analysis (RTCA) (ACEA Bioscience, San Diego, CA, USA) is a test system applied to monitor conditions such as cell adhesion, cell spread, proliferation, cytotoxicity states, cell signaling in real-time. In this system, a noninvasive electrical signal is used for this purpose. Cells are developed on gold electrodes located on the plate floor. Accordingly, a cell index (CI) value is determined in parallel with the impedance changes in the electrodes. These values are transferred to the computer environment, and total impedance graphics are obtained with the help of values [21].

SH-SY5Y cells are grown on 96 well plates at 37 °C with 5% $CO_2$ using the xCELLigence RTCA instrument. To determine the cytotoxicity in the cells, $7.2 \times 10^3$ cells are sown in each plate well. Impedance graphs are obtained by realizing the relevant nanoparticle applications and recording *CI* values for 48 h in real-time.

## Statistical analysis

SPSS (version 13.0, SPSS, Chicago, IL, USA) software was used to perform statistical analysis. Accordingly, Duncan's test was used. The purpose of this use is to determine whether the practices performed show significantly different characteristics from the control groups or from each other. Statistical data were determined according to a 0.05 significance level.

# Results

## Characterization of the synthesized MgS NPs

### Surface characterization of MgS NPs

Chemical and mineralogical compositions of synthesized green MgS NPs were determined by scanning electron microscopy (SEM) and Transmission Electron Microscopy (TEM). For SEM analysis, images of MgS NPs were magnified ×10,000 by Zeiss, Active area 10 mm² (Fig. 1a).

Scanning electron microscopy (SEM) Fig. 1 depicted the SEM image of the MgS NPs. The shape of the MgS NPs was a nearly spherical arrangement on the smooth surface which bound parallel together as a small layer formation with the diameter in the range of $25–40 \pm 2.2$ nm and having an average diameter of $60 \pm 2.5$ nm. The present vegetable green synthetic approach afforded the use of a simpler reducing agent, which was non-hazardous, low-cost for the formation of single-phase MgS NPs.

### XRD of MgS NPs

MgS NPs' XRD, which was produced in its peroxidase enzyme catalyst, and its crystallographic analysis was given in Fig. 2. Characteristic peaks that belong to the XRD spectrum in it's at $2\theta = 45.45^\circ$ could be indexed at (220).

### Fourier transform infrared spectroscopy (FTIR) analysis

Fourier transform infrared spectroscopy (FTIR) was used to identify possible biomolecules responsible for the reduction of MgS NPs by green synthesis. Figure 3 showed the FTIR spectrum of MgS NPs synthesized using *Punica granatum* plant extract and $Na_2S$ (Table 1). Spectra showed bands at 3363.5, 1658, 1552, 1440, 1099 and 601 $cm^{-1}$. The sharp band at 1658 $cm^{-1}$ represented the C=O vibrations typical of the structure of flavonoids that could be found in *Punica granatum*. The absorption band at 1398 $cm^{-1}$ releateed to the –C–H bending vibrations in the aromatic amine groups in the flavonoid structure. The peak observed around 1099 $cm^{-1}$ indicates the presence
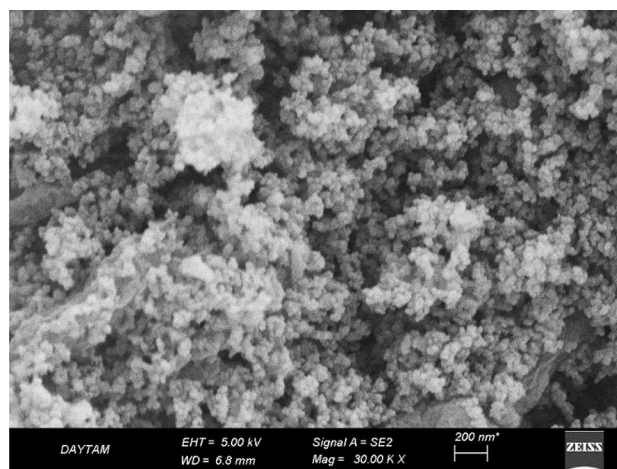


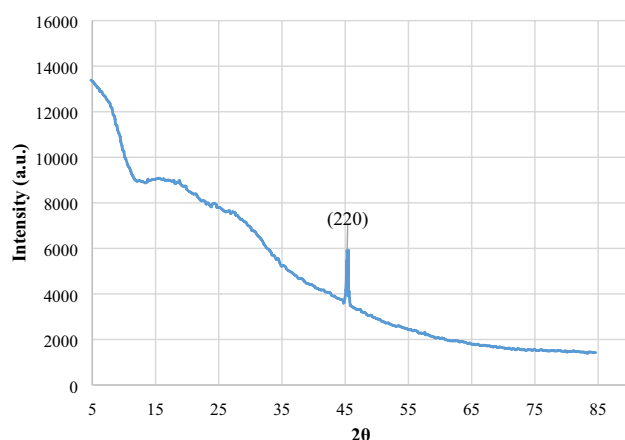**Fig. 1** Scanning electron microscopy and transmission electron microscopy images of MgS NPs

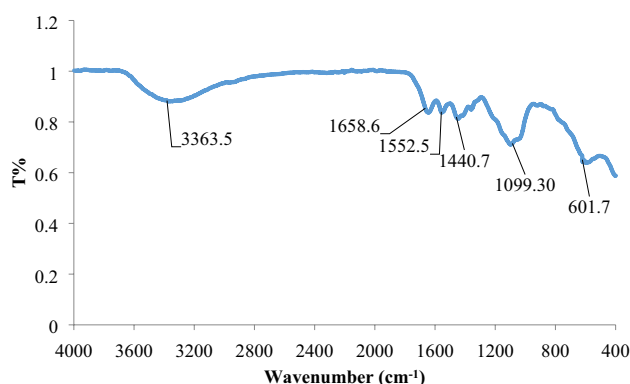Fig. 2 X-ray diffraction pattern of MgS NPs



Fig. 3 Fourier-transform infrared spectrum of MgS NPs

Table 1 Analysis results of bonds in FTIR analysis

| Functional groups and bonds | The characteristic adsorption signals (cm$^{-1}$) |
| --- | --- |
| –CH$_2$ | 601.7 |
| S–C | 1099.30 |
| C–O | 1140.7 |
| C–O–H | 1099.30 |
| –C–H | 1398.24 |
| –C=O | 1658.6 |
| O–H | 3363.5 |

of MgS NPs and characteristic peaks of the C–S bond structure. The observed peak at 601.7 cm$^{-1}$ belonged to the –CH$_2$ group in the aliphatic chain structure. The FTIR spectrum confirmed the presence of bioactive compounds contained in the *Punica granatum* plant [22].

### Results of antitumor effects of CSP + MgS NPs bio-conjugate

In this study, the antitumor effect of CSP + MgS NPs bio-conjugate systems were evaluated. For this purpose, Cisplatin (5 mg/mL) was kept constant and conjugated with different concentrations of MgS NPs and the related reactions were given in the equation below (I). As can be seen, thanks to the nucleophilic reaction with the –Cl groups in the Cisplatin structure, it is attached to Pt in the Cisplatin structure as a challenge. In addition, it is thought that the non-bonded electrons in the MgS structure would interact with the NH$_3$ groups in the Cisplatin structure and that the MgS NPs are connected not only covalently to the Cisplatin structure with weak Wander roller bonds (I).

### Morphologic determination of MgS NPs

Images of SH-SY5Y cell line obtained by inverted microscope are given in Fig. 4. When the images are examined, it may be mentioned that there is a deterioration in the visuality of the cells due to increased cell death. In parallel with increasing MgS NPs doses, it is thought that mass cell deaths increase, and this causes the image to lose its clarity (Fig. 4).

### MTT assay results

To investigate the cytotoxic effects of MgS NPs on the neuroblastoma cell line, a colorimetric method, MTT assay, was performed. Accordingly, all the doses administered after 24 h of exposure were encountered, with the death of cells equivalent to or greater than cisplatin, the positive control. A cell death equivalent to cisplatin, a neuroblastoma drug, was observed at the lowest dose of 10 µg/mL. It was noted that the effectiveness of MgS NPs increased with increasing doses, and the cytotoxic effect on the cancer line became more pronounced.

The highest anticancer efficacy dose of MgS NPs was determined as 75 µg/mL. It is seen that the rate of cancer cells in this dose has decreased by up to 48.54%. According to the data obtained, it has been determined that all doses of MgS NPs are effective, but the most effective results are in the range of 50 to 100 µg/mL. According to the results of MTT analysis, the lowest effective dose was determined as 10 µg/mL compared to other doses and control. The closest effect of this dose was detected at 25 µg/mL. It has been found that these two applications decrease cell viability by 78.64% to 75.37%, respectively.

Bioconjugated nanoparticles, neuroblastoma SH-SY5Y cells have been found to reduce the dose-dependent viability of the neuroblastoma SH-SY5Y cells and the inhibition concentration results ($IC_{50}$) are approximately 63.59 µg/mL (Fig. 5a).
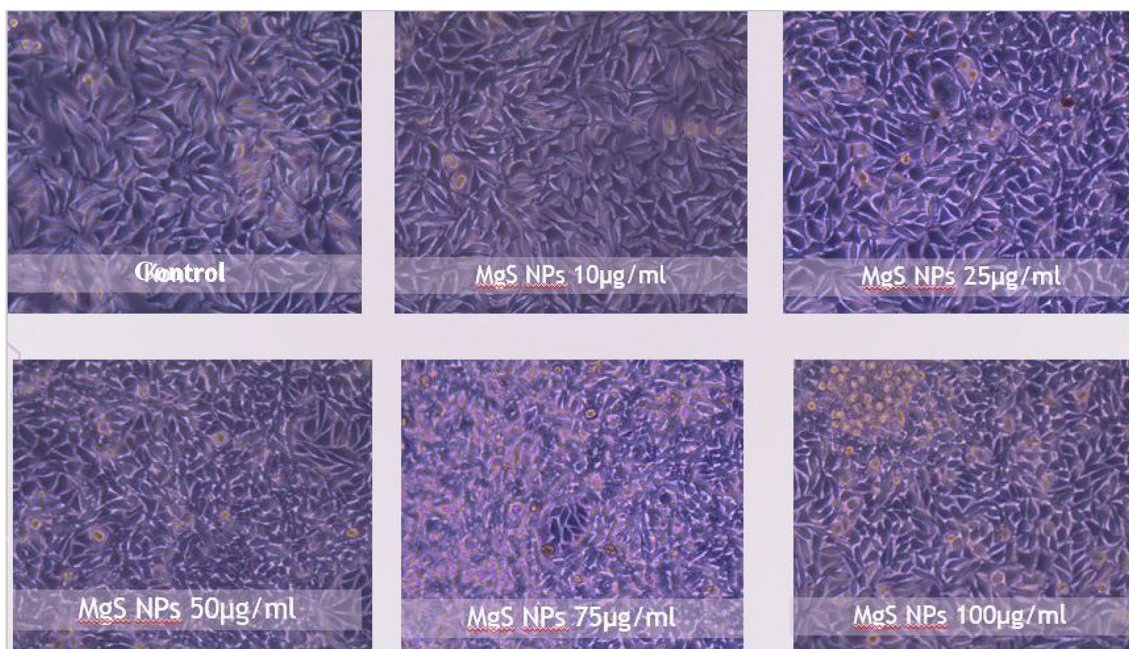
**Fig. 4** Reverse microscope image cisplatin-MgS bioconjugate NPs on cell viability of SH-SY5Y cancer cells

## TOS assay results

The general working principle of the TOS kit is this; the oxidant molecules in the sample oxidize the ferrous-ion chelating complex to the ferric ion. Ferric ion, which is the result of oxidation reaction, forms a colored complex with chromogen in a highly acidic environment. Oxidant density is determined by measuring the color density formed spectrophotometrically.

When the total oxidant status test data are examined, it can be seen that the total oxidant activity increases, especially in high doses of applied MgS NPs. Accordingly, TOS data at doses of 75 to 100 μg/mL were determined as 5.07 and 5.62, respectively. Even in Cisplatin applied neuroblastoma cells, this rate was recorded as 2.62 (Fig. 5b). It can be said that almost all of the TOS data displays dose-dependent oxidant activity increase.

## TAC assay results

TAC kit was applied on the medium taken from the wells 24 h after the drug administration. Absorbance was observed at 660 nm after the dwell time. Considering the TAC levels based on Trolox equiv/mmol/l data, it was observed that the antioxidant activity was quite low at doses of 75 and 100 μg/mL. These data were determined as 1.14 and 1.27 Trolox equiv/mmol/L, respectively. It was observed that the antioxidant activity of MgS NPs at lower doses was higher compared to higher doses. Compared to control and positive control, it

was determined that high doses of MgS NPs have very low antioxidant activity (Fig. 5c).

## Real-time cell cytotoxicity assay

According to the xCELLigence real-time cell viability analysis study, the dose of 75 μg/mL from the MgS NPs, bioconjugates applied showed the most effective result. It has been determined that the applications performed show a relatively dose-dependent effect. Unlike MTT results, it was determined that MgS NPs doses produced results close to each other. According to the data obtained, a 75 μg/mL administration dose has been shown to reduce cell viability by up to 65.95%. It was determined that the dose of 100 μg/mL decreased the cell viability to 66.82% and a dose of 50 μg/mL to 67.38% (Fig. 6.).

Cell index the graph was obtained in accordance with xCELLigence real-time analysis data. In the graph, cell index data in which nanoparticles were applied that varies over time between 26th and 72nd h were given. In Fig. 6, it was seen that the dose of 75 μg/mL reached the lowest cell index data together with 100 μg/mL. It was determined that all of the NPs constructed applied ended the experiment with lower cell index values than cisplatin.

## Discussion

Cisplatin is widely used in the treatment of bladder, lung, ovarian, head, neck, and testicular cancers. It is also known to have an effect on carcinomas, lymphomas, sarcomas, and

**Fig. 5** MTT test results (**a**), Total oxidant status (TOS) test values read spectrophotometrically at 530 nm in cell culture fluid (**b**), Total antioxidant capacity test values read spectrophotometrically at 660 nm in cell culture fluid (**c**) for the Cisplatin-MgS bioconjugate NPs
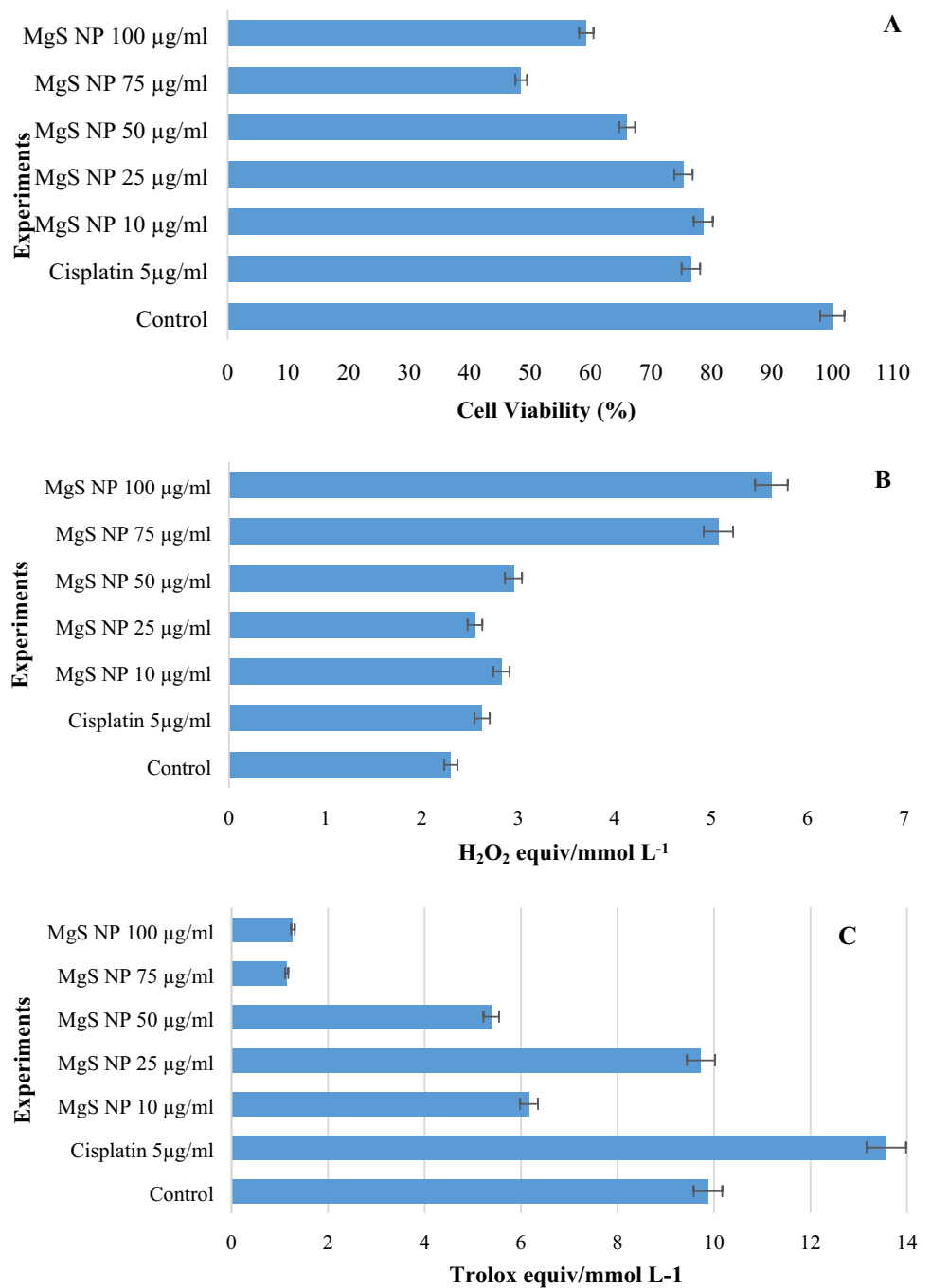


germ cell tumors, and shows an apoptotic effect on cancer cells through mats [23]. The cytotoxic effect caused by cisplatin is due to its covalent attachment to the purine base in the DNA structure.

This DNA damage results in nephrotoxicity, hepatotoxicity, ototoxicity, gastrotoxicity, cardiotoxicity, myelosuppression, allergic reactions, and toxic effects on some reproductive functions [24, 25].

The green synthesis of NPs synthesized by the use of herbal substances is of great importance in the preparation of metal sulfide NPs, due to their non-toxic, non-dangerous, cost-effective, and environmentally friendly properties. In addition, NPs obtained by plant-based green synthesis are more biocompatible than chemically synthesized. In green synthesized NPs groups, this property is due to the closure of biomolecules with certain metal oxide crystals or metals [16, 26]. NPs produced by bioengineering have many useful properties of strong candidates for anticancer drugs or drug distributions [27].
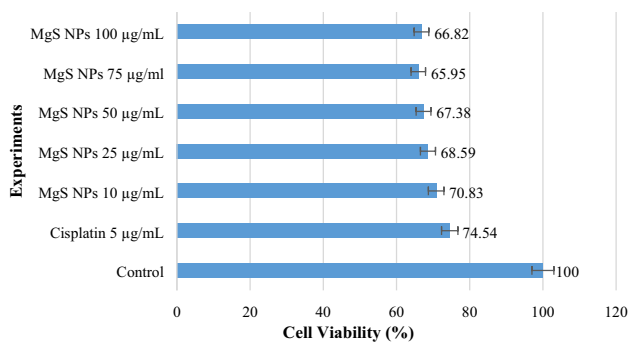
**Fig. 6** Results of cell viability from xCELLigence real-time cell viability analysis

The detection of apoptosis or programmed cell death is important in detecting many health problems, especially cancer, and developing disease-related therapy. Over the years, a number of methods have been discovered and developed for detecting apoptosis. There are several standard techniques such as electron microscopy, TUNEL testing, and flow cytometry. In addition, new techniques such as microfluidic devices, single-molecule spectroscopy, and electrochemical methods are rapidly emerging. These assays measure different parameters associated with apoptotic progression. The MTT test is a colorimetric analysis to evaluate cell metabolic activity as living cells with active metabolism convert MTT to a purple colored formazan product [28]. According to the MTT results obtained, it was determined that MgS NPs at 75 μg/mL dose showed a cytotoxic effect on the neuroblastoma cancer line by reducing 51.46% viability. This rate was much more than the effectiveness of cisplatin, a drug that is included in the standard treatment of neuroblastoma cancer line. MgS NPs exhibited toxicity on neuroblastoma cancer cells more effectively than cisplatin. There was no study in the literature investigating the effect of MgS NPs on neuroblastoma cancer line. However, studies with MgO NPs showed that there was a cytotoxic effect on HepG2, BJ cell lines, [29] while there was no significant cell toxicity on the SH-SY5Y cell line [30].

The reason for the preference of the neuroblastoma cell line to investigate the anticancer efficacy of cisplatin-conjugated MgS NPs was that it was the most common type of cancer in infants. Individual chromosome abnormalities occurring in the tumor complicated the treatment of neuroblastoma. For this reason, there was a need for a comprehensive treatment method that would affect all neuroblastoma cancers, independent of chromosomal abnormalities. In this study, the neuroblastoma cell line was selected for this reason [31]. The synthesized nanoparticles achieved a rate of 51.46% success in the standard SH-SY5Y series. Preliminary data required for the investigation of the relevant nanoparticles on cancer lines containing chromosomal abnormalities were obtained.

The highest oxidant activity was found at doses of 75 and 100 μg/mL, which are the two most effective doses of MgS NPs in terms of anticancer activity. It was believed that the applied nanoparticle structures stimulate cancer cells to produce reactive oxygen species. Behzadi et al. [15] was similarly determined that MgS NPs structures was showed an effect by increasing oxidative stress compared to control on a different cancer line. It is thought that the data obtained in this direction comply with the literature, and the resulting oxidant activity may be due to the Mg$^{2+}$ ion contained in the nanoparticle content. The excessive oxidant activity exhibited by the applied MgS NPs on the cancer line gives an idea about the mechanism of the anticancer activity exhibited by the nanoparticles [32, 33].

It is clearly seen that in the applications of MgS NPs compared to the control, especially in doses of 75 and 100 μg/mL, where the anticancer efficacy is greatest, the antioxidant effectiveness is decreased. Increased antioxidant activity in neuroblastoma cells treated with cisplatin is consistent with the data obtained from the literature [34]. It is not known whether nanostructures acting on the neuroblastoma cancer line and cisplatin differ in antioxidant activity. However, in studies with different nanoparticles, it has been noted that it does not change the level of antioxidant activity TAC in cancer lines [35]. Besides, this study underlined that the study has integrity due to the increase in the oxidant level and the decrease in the antioxidant status in the application groups exhibiting anticancer activity. There is no MgS NPs synthesis in the literature. It is clear that this study will lead the literature in terms of the first synthesis of MgS NPs and the first attempt on SH-SY5Y cell line by creating a bioconjugate with Cisplatin.

The results obtained showed that; NPs bioconjugates applied were relatively more effective than cisplatin on SH-SY5Y cell line. By extending the observation period of the applications, data similar to MTT data could be obtained. Obtaining the results in a relatively dose-dependent manner indicateed that xCELLigence correlates with MTT data. The data obtained from the cell index graph, which expresses the change of the number of cells over time, was confirmed. All of the applied nanoparticle structures showed effective results from cisplatin. According to cell index data, the most effective doses of NPs constructs, which were found to decrease cell viability compared to both control and cisplatin, were 75 and 100 μg/mL. Accordingly, it was determined that 75 μg/mL bioconjugate dose was acceptable as a new treatment approach that could be evaluated in highly aggressive cancer type neuroblastoma.

## Conclusions

As a result, it was clear that MgS NPs and MgS NPs bioconjugates Cisplatin, synthesized and characterized by the green synthesis method, had a greater effect on the neuroblastoma cancer line than Cisplatin drug. It was thought that this dose-dependent effect could be caused oxidative stress by increasing the types of reactive oxygen in the cancer cell. In addition, the MTT assay and xCELLigence assay results also showed that the anticancer effects of MgS NPs bioconjugates Cisplatin were more effective against the SH-SY5Y neuroblastoma cell line using a lower total drug dose, while drug retention in nanoparticles further reduced systemic exposure and toxicity. Although MgS NPs bioconjugates tested in a neuroblastoma model by experiments with Cisplatin prodrug formulation, it was thought to be effective in the treatment of aggressive and malignant tumors. Accordingly, it was estimated that future studies could be quite effective in determining the mechanism of action of nanoparticles.

## Compliance with ethical standards

**Conflict of interest** The authors declare that there are no conflicts of interest regarding the publication of this study.

**Ethical approval** This article does not contain any studies with human participants or animals performed by any of the authors.

## References

1. El-Sayed MA (2001) Some interesting properties of metals confined in time and nanometer space of different shapes. Acc Chem Res 34(4):257–264. https://doi.org/10.1021/ar960016n
2. Dos Santos Ramos MA, Da Silva PB, Sposito L, De Toledo LG, Bonifacio BV, Rodero CF, Dos Santos KC, Chorilli M, Bauab TM (2018) Nanotechnology-based drug delivery systems for control of microbial biofilms: a review. Int J Nanomed 13:1179–1213. https://doi.org/10.2147/ijn.S146195
3. Orbaek White A, McHale M, Barron A (2015) Synthesis and characterization of silver nanoparticles for an undergraduate laboratory. J Chem Educ 92:339–344. https://doi.org/10.1021/ed500036b
4. Nadaroglu H, Gungor AA, Ince S, Babagil A (2017) Green synthesis and characterization of platinum nanoparticles using quail egg yolk. Spectrochim Acta Part A Mol Biomol Spectrosc 172:43–47. https://doi.org/10.1016/j.saa.2016.05.023
5. Abdal Dayem A, Hossain MK, Lee SB, Kim K, Saha SK, Yang GM, Choi HY, Cho SG (2017) the role of reactive oxygen species (ROS) in the biological activities of metallic nanoparticles. Int J Mol Sci. https://doi.org/10.3390/ijms18010120
6. Satapathy SR, Mohapatra P, Preet R, Das D, Sarkar B, Choudhuri T, Wyatt MD, Kundu CN (2013) Silver-based nanoparticles induce apoptosis in human colon cancer cells mediated through p53. Nanomedicine (London, England) 8(8):1307–1322. https://doi.org/10.2217/nnm.12.176
7. Fageria L, Pareek V, Dilip RV, Bhargava A, Pasha SS, Laskar IR, Saini H, Dash S, Chowdhury R, Panwar J (2017) Biosynthesized protein-capped silver nanoparticles induce ROS-dependent proapoptotic signals and prosurvival autophagy in cancer cells. ACS Omega 2(4):1489–1504. https://doi.org/10.1021/acsomega.7b00045
8. Guo D, Zhu L, Huang Z, Zhou H, Ge Y, Ma W, Wu J, Zhang X, Zhou X, Zhang Y, Zhao Y, Gu N (2013) Anti-leukemia activity of PVP-coated silver nanoparticles via generation of reactive oxygen species and release of silver ions. Biomaterials 34(32):7884–7894. https://doi.org/10.1016/j.biomaterials.2013.07.015
9. Ahamed M, Akhtar MJ, Raja M, Ahmad I, Siddiqui MK, AlSalhi MS, Alrokayan SA (2011) ZnO nanorod-induced apoptosis in human alveolar adenocarcinoma cells via p53, survivin and bax/bcl-2 pathways: role of oxidative stress. Nanomed Nanotechnol Biol Med 7(6):904–913. https://doi.org/10.1016/j.nano.2011.04.011
10. Wang N, Cheng X, Li N, Wang H, Chen H (2019) Nanocarriers and their loading strategies. Adv Healthcare Mater 8(6):e1801002. https://doi.org/10.1002/adhm.201801002
11. London WB, Castleberry RP, Matthay KK, Look AT, Seeger RC, Shimada H, Thorner P, Brodeur G, Maris JM, Reynolds CP, Cohn SL (2005) Evidence for an age cutoff greater than 365 days for neuroblastoma risk group stratification in the Children's Oncology Group. J Clin Oncol 23(27):6459–6465. https://doi.org/10.1200/jco.2005.05.571
12. Applebaum MA, Vaksman Z, Lee SM, Hungate EA, Henderson TO, London WB, Pinto N, Volchenboum SL, Park JR, Naranjo A, Hero B, Pearson AD, Stranger BE, Cohn SL, Diskin SJ (2017) Neuroblastoma survivors are at increased risk for second malignancies: a report from the international neuroblastoma risk group project. Eur J Cancer 72:177–185. https://doi.org/10.1016/j.ejca.2016.11.022
13. Jung J (2014) Human tumor xenograft models for preclinical assessment of anticancer drug development. Toxicol Res 30(1):1–5. https://doi.org/10.5487/tr.2014.30.1.001
14. Teitz T, Stanke JJ, Federico S, Bradley CL, Brennan R, Zhang J, Johnson MD, Sedlacik J, Inoue M, Zhang ZM, Frase S, Rehg JE, Hillenbrand CM, Finkelstein D, Calabrese C, Dyer MA, Lahti JM (2011) Preclinical models for neuroblastoma: establishing a baseline for treatment. PLoS ONE 6(4):e19133. https://doi.org/10.1371/journal.pone.0019133
15. Behzadi E, Sarsharzadeh R, Nouri M, Attar F, Akhtari K, Shahpasand K, Falahati M (2018) Albumin binding and anticancer effect of magnesium oxide nanoparticles. Int J Nanomed 14:257–270. https://doi.org/10.2147/ijn.S186428
16. Nadaroglu H, Alayli A, Ince S (2017) Synthesis of nanoparticles by green synthesis method. Int J Innov Res Rev 1:6–9
17. Nadaroglu H, Onem H, Alayli Gungor A (2017) Green synthesis of $Ce_2O_3$ NPs and determination of its antioxidant activity. IET Nanobiotechnol 11(4):411–419. https://doi.org/10.1049/iet-nbt.2016.0138
18. Alaylı Güngör AN, Gültekin D (2019) Synthesis and characterization of nano-strontium oxide (SrO) using erzincan cimin grape (Vitis vinifera, Cimin). Chem Sci Int J 26(3):1–7. https://doi.org/10.9734/CSJI/2019/v26i330092
19. Groh T, Hrabeta J, Abdel-Rahman M, Doktorova-Marikova H H, Eckschlager T, Stiborová M (2015) The synergistic effects of DNA-damaging drugs cisplatin and etoposide with a histone deacetylase inhibitor valproate in high-risk neuroblastoma cells. Int J Oncol 47(1):343–352. https://doi.org/10.3892/ijo.2015.2996
20. Erel O (2005) A new automated colorimetric method for measuring total oxidant status. Clin Biochem 38(12):1103–1111. https://doi.org/10.1016/j.clinbiochem.2005.08.008
21. Morgan K, Gamal W, Samuel K, Morley SD, Hayes PC, Bagnaninchi P, Plevris JN (2019) Application of impedance-based

techniques in hepatology research. J Clin Med. https://doi.org/10.3390/jcm9010050

22. Dobrucka R (2016) Synthesis of MgO nanoparticles using artemisia abrotanum herba extract and their antioxidant and photocatalytic properties. Ir J Sci Technol Trans A Sci 42(2):547–555. https://doi.org/10.1007/s40995-016-0076-x

23. Dasari S, Tchounwou PB (2014) Cisplatin in cancer therapy: molecular mechanisms of action. Eur J Pharmacol 740:364–378. https://doi.org/10.1016/j.ejphar.2014.07.025

24. Hartmann JT, Fels LM, Knop S, Stolt H, Kanz L, Bokemeyer C (2000) A randomized trial comparing the nephrotoxicity of cisplatin/ifosfamide-based combination chemotherapy with or without amifostine in patients with solid tumors. Invest New Drugs 18(3):281–289. https://doi.org/10.1023/a:1006490226104

25. Hartmann JT, Lipp HP (2003) Toxicity of platinum compounds. Expert Opin Pharmacother 4(6):889–901. https://doi.org/10.1517/14656566.4.6.889

26. Ali ZA, Roslan MA, Yahya R, Wan Sulaiman WY, Puteh R (2017) Eco-friendly synthesis of silver nanoparticles and its larvicidal property against fourth instar larvae of *Aedes aegypti*. IET Nanobiotechnol 11(2):152–156. https://doi.org/10.1049/iet-nbt.2015.0123

27. Lojk J, Repas J, Veranič P, Bregar VB, Pavlin M (2020) Toxicity mechanisms of selected engineered nanoparticles on human neural cells in vitro. Toxicology 432:152364. https://doi.org/10.1016/j.tox.2020.152364

28. Henslee EA, Torcal Serrano RM, Labeed F, Jabr RI, Fry CH, Hughes MP, Hoettges KF (2016) Accurate quantification of apoptosis progression and toxicity using a dielectrophoretic approach. Analyst 141:6408–6415

29. Lai MB, Jandhyam S, Dukhande V, Bhushan A, Daniels C, Leung S, Lai J (2009) Cytotoxicity of metallic oxide nanoparticles in human neural and non-neural cells. Technical proceedings of the 2009 NSTI nanotechnology conference and Expo. NSTI-Nanotechnology 2:135–138

30. Hasbullah N, Mat zain M, Kamarulzaman N (2013) Nanotoxicity of Magnesium Oxide on Human Neuroblastoma SH-SY5Y Cell Lines. Adv Mater Res 667:160–164. https://doi.org/10.4028/www.scientific.net/AMR.667.160

31. Whittle SB, Smith V, Doherty E, Zhao S, McCarty S, Zage PE (2017) Overview and recent advances in the treatment of neuroblastoma. Expert Rev Anticancer Ther 17(4):369–386. https://doi.org/10.1080/14737140.2017.1285230

32. Pandurangan M, Veerappan M, Kim D (2014) Cytotoxicity of zinc oxide nanoparticles on antioxidant enzyme activities and mRNA expression in the cocultured $C_2C1_2$ and 3T3-L1 cells. Appl Biochem Biotechnol 175:1270–1280. https://doi.org/10.1007/s12010-014-1351-y

33. Vega-Jiménez AL, Vázquez-Olmos AR, Acosta-Gío E, Álvarez-Pérez, MA (2019) In vitro antimicrobial activity evaluation of metal oxide nanoparticles. In: Kai Seng Koh VLW (ed) Nanoemulsions—properties, fabrications and applications. IntechOpen, London

34. Olas B, Wachowicz B, Majsterek I, Blasiak J (2005) Resveratrol may reduce oxidative stress induced by platinum compounds in human plasma, blood platelets and lymphocytes. Anticancer Drugs 16(6):659–665. https://doi.org/10.1097/00001813-200507000-00011

35. Aydin N, Arslan M, Sonmez E, Türkez H (2017) Cytotoxicity analysis of tellurium dioxide nanoparticles on cultured human pulmonary alveolar epithelial and peripheral blood cell cultures. Biomed Res (India) 28:3300–3304